Department of Physics and Astronomy
University of Heidelberg

Bachelor Thesis in Physics
submitted by

Ferdinand Gleixner
born in Tettnang (Germany)
November 8th 1995

Parametric instabilties of short and ultra-intense laser pulses in a plasma

This Bachelor Thesis has been carried out by Ferdinand Gleixner at the
Max-Planck-Institut für Kernphysik in Heidelberg
under the supervision of
Honorarprof. Christoph H. Keitel

Abstract

Parametric instabilities in laser-plasma interactions are investigated in the ultra-relativistic regime, including the leading-order term of the Landau-Lifshitz radiation reaction equation. After a detailed exploration to the theory of parametric instabilities, the effects of the radiation reaction force on the growth rate are discussed by comparing to the results without radiation reaction force. The radiation reaction force leads to merging of the two Raman branches and also excites new modes, e.g. the so-called quasi-modes. Furthermore the radiation reaction force increases the endurance of the short wavelength perturbations. Increased endurence affects the quality of the laser pulse shape, which is important particularly for experiments, which require a precisely-shaped laser pulse.

Zusammenfassung

Der Einfluss der Strahlungsrückwirkung auf parametrische Instabilitäten in Laser-Plasma Interaktionen wird, unter Berücksichtigung des Terms erster Ordnungs der Landau-Lifschitz Gleichung, untersucht. Einem detaillierten Theorieteil folgt die Untersuchung der Effekte der Strahlungsrückwirkung unter anderem auf die Wachstumsrate der Instabilität. Um den Einfluss festzustellen werden diese mit den Ergebnissen ohne diese Erweiterung verglichen. Das Einbinden der Strahlungsrückwirkung führt zu einem Verschmelzen der beiden Raman Zweige und regt neue Moden, u.a. die Quasi-Moden an. Die Strahlungsrückwirkung zeigt, dass auch kurzwelligere Wellenlängen Instabilitäten im Plasma anregen können. Dies hat einen bedeutenden Einfluss auf Experimente, die einen in der Form wohldefinierten Laserpuls benötigen.

Contents

1 Introduction

The area of high-power laser-plasma interaction covers a broad area of research ranging from medical physics, new X-ray sources, next generation of compact particle accelerators and laser-driven fusion [1, 2, 3, 4, 5]. The underlying advantage of using the high-power laser-plasma interaction is to substantially reduce the size and cost of installations required for above-mentioned applications.

The most interesting part of the theory of laser-plasma interactions are the parametric instabilities. These instabilities belong to the class of nonlinear physics problems where the coefficients of a second-order differential equation are time dependent. For example, motion of a pendulum, whose length varies with time, or a child on a swing. When the child on a moving swing sits up and down, the centre of mass of the child oscillates with time, making it a simple pendulum whose effective length varies with time. Thus, the motion of swing becomes unstable and leads to higher and higher swing motion, as one might have experienced it in childhood.

In the context of laser-plasma interaction, parametric instabilities arise due to coupling of the electron oscillatory motion with the plasma oscillations and are driven by ponderomotive and relativistic effects [4, 1, 6, 7]. The stimulated Raman scattering (SRS) is one of the most prominent examples for a parametric instability. In SRS, a pump laser scatters into two daughter waves propagating in the same direction as the parent wave (Forward Raman scattering or FRS) or into a single backward moving daughter wave (Backward Raman scattering or BRS). The frequency of those waves is either upshifted, which is called anti-Stokes mode, or downshifted, which is called Stokes mode. The results and the technique used for the solution of parametric instabilities could also be applied to other problems of nonlinear physics.

There have been constant efforts to increase the intensities of the short-pulse lasers around the world. With the commissioning of the Extreme Light Infrastructure (ELI) project in Europe [8], laser pulse with intensity $I_l \gg 10^{22}\mathrm{W/cm}^2$ will be available soon. In this ultra-relativistic regime of laser-plasma interaction, radiation reaction force plays an important role [9, 10]. Inclusion of radiation reaction force in the plasma dynamics pushes the parametric instability research into hitherto unexplored regime where several novel effects are expected to occur [7].

This thesis focuses on the inclusion of radiation reaction force in the plasma dynamics. After describing the theory of the parametric instabilities in relativistic and ultra-relativistic regimes, the generalised dispersion relations for the modulational interactions in these regimes are derived and numerically solved. MATLAB code is developed especially for this purpose to correctly identify different branches of the unstable modes in the plasma. I plot various quantities e.g. growth rates, maximum wavevectors and unstable branches in plasmas for a wide range of laser-plasma parameters, with and without the radiation reaction force to identify the influence of it on the parametric instabilities. Afterwards the physical implications of the results are discussed and I summarise the findings in the last chapter. The appendix includes the MATLAB code used in this thesis with a few explanations.

2 Theory of parametric instabilities

The mathematical analysis of the instabilities firstly follows the books by Kruer[4] and Gibbon[1]. For the inclusion of radiation reaction using Landau-Lifshitz equation the calculations of Kumar et al. are followed [7]. To give a detailed overview how the dispersion relation could be derived from the Vlasov equation, the analysis is described in detail. This is firstly done in the non-relativistic regime and afterwards in the relativistic regime. Also a detailed overview for the growth rate of the plasma mode and the frequency mismatches of Stokes and anti-Stokes mode in Raman scattering are given. The last part of the theory section is the calculation of the dispersion relation taking the radiation reaction force into account.

2.1 Two-fluid description and the dispersion relation of plasma waves

A plasma consists of two different types of particles. The heavy positive charged ions and the less massive electrons. A collisionless plasma is assumed, so the mean free path between particles is larger than the wavelength of the oscillations in the plasma, which leads to the fact that collision of plasma particles can be neglected. The spot size of the pump laser is much larger than the wavelength of this laser, so a plane-wave assumption for the pump laser can be made. If the spot size would be of the order of wavelength a plane-wave approximation could not be made. Only a short puls excitation would occur.

The first equation on the way to the dispersion relation is the Vlasov equation, which describes the evolution of a collisionless plasma:

$$\frac{\partial f_j}{\partial t} + \mathbf{v} \cdot \frac{\partial f_j}{\partial \mathbf{x}} + \frac{q_j}{m_j} \left(\mathbf{E} + \frac{\mathbf{v}}{c} \times \mathbf{B} \right) \frac{\partial f_j}{\partial \mathbf{v}} = 0, \tag{1}$$

with a phase space distribution function $f_j(\mathbf{x}, \mathbf{v}, t)$, the magnetic respectively electric field $\mathbf{B}$ and $\mathbf{E}$ as well as the charge and mass of the particles q_j, m_j. From this equation can be seen that the phase-space density changes on a dynamical trajectory. By deriving the moments of this equation a fluid-like approximation for the components of a plasma is obtained. Now assuming a cold plasma approximation as well as a short pulsed laser, leads to the consideration that the electrons move quickly while the ions more or less stay at their positions leading to a constant background (Zn_{0i} with the charge state of the ions Z and the density n_{0i}). For this the electron motion can be assumed to be the main part of the high frequent density fluctuations.
Using Maxwell's equations the following force equation (3) is derived from the moments equations as well as neglecting the Lorentz-force. For the description of the dynamics in a collisonless cold plasma the continuity equation, the force equation and the adiabatic equation are necessary:

$$\frac{\partial n_e}{\partial t} + \nabla(n_e \mathbf{v}_e) = 0, \tag{2}$$

$$\frac{\partial}{\partial t}(n_e \mathbf{v}_e) + \nabla(n_e {\mathbf{v}_e}^2) = -\frac{n_e e \mathbf{E}}{m_e} - \frac{1}{m_e} \nabla \mathbf{p}_e, \tag{3}$$

$$\frac{\mathbf{p}_e}{{n_e}^3} = \text{constant} \tag{4}$$

where e is the charge of an electron, m_e is the electron mass, n_e is the electron density, v_e is the mean thermal velocity of the electrons and p_e is the electron pressure. After derivation by time of continuity equation (2) and inserting into the spatial derivation of the force equation (3) using the symmetry of second derivatives it is obtained:

$$\frac{\partial^2}{\partial t^2} n_e - \nabla^2(n_e {\mathbf{v}_e}^2) - \frac{e}{m_e}\nabla(n_e \mathbf{E}) - \frac{1}{m_e}\nabla^2 \mathbf{p}_e = 0. \tag{5}$$

Using the Poisson equation the electric field can be related to the density distribution:

$$\nabla \mathbf{E} = -4\pi e(n_e - Z n_{0i}). \tag{6}$$

The next step is to linearise the equations ($n_e = n_0 + \delta e, p_e = \Sigma_e + \delta p, v_e = v_0 + \delta v$, with perturbation of the quantities δ it is assumed $v_0 = 0$). The result of this linearization is:

$$\nabla(\delta \mathbf{E}) = -4\pi e \delta n, \tag{7}$$

$$\delta \mathbf{p} = 3m{\mathbf{v}_e}^2 \delta n, \tag{8}$$

$$\frac{\partial^2}{\partial t^2}\delta n - \frac{n_e}{m_e}\delta \mathbf{E} - \frac{\partial^2}{\partial x^2}\delta \mathbf{p} = 0. \tag{9}$$

Now taking a wavelike ansatz for every component (δn, $\delta \mathbf{E}$, $\delta \mathbf{p}$, $\delta \mathbf{v} \sim e^{-i(wt-kx)}$) the plasma oscillations can be described with:

$$\left(\frac{\partial^2}{\partial t^2} - 3{\mathbf{v}_e}^2\nabla^2 + {\omega_{pe}}^2\right)\delta n = 0, \tag{10}$$

with $\omega_{pe} = (4\pi e^2 n_0/m_e)^{1/2}$ the electron plasma frequency with electron density $n_0 = Z n_{0i}$. From the fourier-analysis of equation (10) the dispersion relation for the plasma wave becomes:

$$\omega^2 = {\omega_{pe}}^2 + 3k^2 {v_e}^2. \tag{11}$$

The frequency of this wave is mostly ω_{pe} with a small thermal correction depending on the wavenumber.

2.2 Dispersion relation of parametric instabilities in a plasma

If the pressure term is now neglected instead of the Lorentz force in equation (3) the new force equation is:

$$\frac{\partial}{\partial t}(n_e \mathbf{v}_e) + \nabla(n_e {\mathbf{v}_e}^2) = -\frac{n_e e}{m_e}\left(\mathbf{E} + \frac{\mathbf{v}}{c} \times \mathbf{B}\right). \tag{12}$$

For more uniform descriptions of the electric and magnetic field the potential notation is used: $\mathbf{E} = -\nabla\Phi - \partial\mathbf{A}/\partial t$ and $\mathbf{B} = \nabla \times \mathbf{A}$ with Φ the electric potential and $\mathbf{A}$ the vector

potential. For the next step Poisson's equation, the vector identity $\mathbf{a} \times (\mathbf{b} \times \mathbf{c}) = \mathbf{b}(\mathbf{a} \cdot \mathbf{c}) - \mathbf{c}(\mathbf{a} \cdot \mathbf{b})$ as well as the following Maxwell equation $\nabla \times (\nabla \times \mathbf{A}) = 4\pi \mathbf{J}/c + 1/c\ \partial \mathbf{E}/\partial t$ are needed. After identifying $\mathbf{J} = \sum_i e_i n_i \mathbf{v}_i$ and using Lorenz gauge ($\nabla \cdot \mathbf{A} = 0$) the resulting dispersion relations are:

$$\omega^2 - {\omega_{pe}}^2 = 0, \tag{13}$$

$$\omega_0{}^2 - \omega_p e^2 - k^2 c^2 = 0. \tag{14}$$

A coupling of these two dispersion relations can be seen by Raman scattering. To describe this it is needed to introduce the ponderomotive force.
The ponderomotive force is the coupling of an electro-magnetic wave into the oscillation of an inhomogeneous plasma. The force equation is:

$$\frac{\partial \mathbf{p}_e}{\partial t} + v_e \nabla p_e = -e \cdot \mathbf{E}(\mathbf{x}, t), \tag{15}$$

$\mathbf{p}_e = m\mathbf{v}_e$ is the momentum of the electrons. Assuming $\mathbf{E}(\mathbf{x}, t) = \mathbf{E}(\mathbf{x}) sin(\omega t)$ the ponderomotive force $\mathbf{F}_p$ is:

$$\mathbf{F}_p = -\frac{e^2}{4 m_e \omega} \nabla \mathbf{E}^2(\mathbf{x}). \tag{16}$$

This force is the reason why a light wave that propagates in a plasma can excite an instability. The ponderomotive force leads to instabilities which can be calculated by Raman scattering. Raman scattering describes the coupling of a pump-light into a scattered light wave plus an electron plasma wave. The first steps to calculate the Raman instabilities is to identify the matching conditions for the wave numbers and frequencies:

$$\omega_0 = \omega_s + \omega_{ek}, \tag{17}$$

$$k_0 = k_s + k, \tag{18}$$

where ω_0 and k_0 are frequency and wavenumber of the incident light wave, and s stands for the same quantities of the scattered light wave. ω_{ek} and k are the frequency and wavenumber of the electron plasma wave. The idea of Raman instability analysis is to use Ampère's law and then separate the current density into a transverse part which describes the light wave and a longitudinal part which describes the electrostatic plasma wave:

$$\nabla \times \mathbf{B} = \frac{4\pi}{c} \mathbf{J} + \frac{1}{c} \frac{\partial \mathbf{E}}{\partial t}. \tag{19}$$

Expressing the field in terms of potential, as well as using Lorenz gauge and vector identities leads to:

$$\left(\frac{1}{c^2} \frac{\partial^2}{\partial t^2} - \nabla^2 \right) \mathbf{A} = \frac{4\pi}{c} \mathbf{J} - \frac{1}{c} \frac{\partial}{\partial t} \Phi. \tag{20}$$

Via Poisson's equation written in terms of potential ($\nabla^2 \Phi = -4\pi\rho$) and the continuity equation $\partial\rho/\partial t + \nabla \mathbf{J} = 0$ the connection between the current $\mathbf{J}$ and the potential Φ is calculated as:

$$\nabla \cdot \left(\frac{\partial}{\partial t} \nabla \Phi - 4\pi \mathbf{J} \right) = 0. \tag{21}$$

Hence $\mathbf{J}_t \sim \mathbf{A}$ it is $\nabla \mathbf{J}_t = 0$ which leads to $\partial(\nabla\Phi)/\partial t = 4\pi \mathbf{J}_l$. Now equation (20) can be written as:

$$\left(\frac{1}{c^2}\frac{\partial^2}{\partial t^2} - \nabla^2\right)\mathbf{A} = \frac{4\pi}{c}\mathbf{J}_t. \tag{22}$$

If furthermore $\mathbf{A} \cdot \nabla n_e = 0$ the transverse current could be expressed by $\mathbf{J}_t = -n_e e \mathbf{v}_t$ with $\mathbf{v}_t$ the oscillation velocity of an electron in an electric field of a light wave if $|\mathbf{v}_t| \ll c$. The transverse velocity can be determined as:

$$\mathbf{v}_t = \frac{e\mathbf{A}}{mc}, \tag{23}$$

because of $\partial \mathbf{v}/\partial t = -\frac{e}{mc}\partial \mathbf{A}/\partial t$. Equation (22) leads to:

$$\left(\frac{1}{c^2}\frac{\partial^2}{\partial t^2} - \nabla^2\right)\mathbf{A} = -\frac{4\pi e}{mc^2} n_e \mathbf{A}. \tag{24}$$

The next step is to linearise this equation via $\mathbf{A} = \mathbf{A}_l + \delta\mathbf{A}$, where $\mathbf{A}_l$ is the large amplitude light wave and $\delta\mathbf{A}$ its perturbation. Also linearising in $n_e = n_0 + \delta n_e$, with background plasma density and its perturbation leads to:

$$\left(\frac{1}{c^2}\frac{\partial^2}{\partial t^2} - \nabla^2\right)(\mathbf{A}_l + \delta\mathbf{A}) = -\frac{4\pi e}{mc^2}(n_0 + \delta n)(\mathbf{A}_l + \delta\mathbf{A}). \tag{25}$$

Hence $\mathbf{A}_l$ and n_0 are taken as constant and all terms containing δ^2 are neglectable:

$$\left(\frac{1}{c^2}\frac{\partial^2}{\partial t^2} - \nabla^2\right)\delta\mathbf{A} = -\frac{4\pi n_0 e}{mc^2}\delta\mathbf{A} - \frac{4\pi(n_0 + \delta n)e}{mc^2}\mathbf{A}_l. \tag{26}$$

Now the plasma frequency can be identified as ${\omega_{pe}}^2 = 4\pi n_0 e/m$ which leads to equation (27) where RHS is the transverse current times the large amplitude light wave:

$$\left(\frac{\partial^2}{\partial t^2} - c^2\nabla^2 + {\omega_{pe}}^2\right)\delta\mathbf{A} = -\frac{4\pi e}{m}\delta n \mathbf{A}_l. \tag{27}$$

Taking again the continuity equation (2) and the pressure neglecting force equation:

$$\frac{\partial}{\partial t}(\mathbf{v}_e) + \mathbf{v}_e \nabla \mathbf{v}_e = -\frac{e}{m_e}\left(-\nabla\Phi + \frac{\mathbf{v}}{c} \times (\nabla \times \mathbf{A})\right), \tag{28}$$

and splitting the velocity into a transverse and a longitudinal part $\mathbf{v}_t$ and $\mathbf{v}_l$ it can be seen that $\mathbf{v}_e = \mathbf{v}_l + e\mathbf{A}/mc$. By using a vector identity and the previous result, the time derivative of the longitudinal velocity becomes:

$$\frac{\partial}{\partial t}\mathbf{v}_l = \frac{e}{m}\nabla\Phi - \nabla\left(\mathbf{v}_l + \frac{e\mathbf{A}}{mc}\right)^2. \tag{29}$$

The second term can be identified as the ponderomotive force. Again linearising the equation the results for equation (2) and equation (29) are:

$$\frac{\partial}{\partial t}\delta n + n_0 \nabla \delta \mathbf{v} = 0, \tag{30}$$

$$\frac{\partial}{\partial t}\mathbf{v} = \frac{e}{m}\nabla\Phi - \frac{e^2}{m^2c^2}\nabla^2\left(\mathbf{A}_l \delta\mathbf{A}\right). \tag{31}$$

Taking the spatial derivative of equation (31) and the time derivative of equation (30) the change of electron density by variation of the electro-magnetic density is:

$$\left(\frac{\partial^2}{\partial t^2} + \omega_{pe}\right)\delta n = \frac{n_0 e^2}{m^2c^2}\nabla^2\left(\mathbf{A}_l \delta\mathbf{A}\right). \tag{32}$$

For further analysis $\mathbf{A}_l = \mathbf{A}_0 \cos(k_0 x - \omega_0 t)$, the fourier-analysis of equation (27) as well as equation (32) are used.
Because of $(\cos(k_0 x - \omega_0 t)) = \frac{1}{2}\left[\delta(k + k_0, \omega + \omega_0) + \delta(k - k_0, \omega - \omega_0)\right]$ it is obtained:

$$(\omega^2 - k^2c^2 - {\omega_{pe}}^2)\delta\mathbf{A}(k, w) = \frac{4\pi e^2}{2m}\mathbf{A}_0\left[\delta n_e(k + k_0, \omega + \omega_0) + \delta n_e(k - k_0, \omega - \omega_0)\right], \tag{33}$$

$$(\omega^2 - {\omega_{pe}}^2)\delta n_e(k, w) = \frac{k^2e^2n_0}{2m^2c^2}\mathbf{A}_0\left[\delta\mathbf{A}(k + k_0, \omega + \omega_0) + \delta\mathbf{A}(k - k_0, \omega - \omega_0)\right]. \tag{34}$$

To finally derive the dispersion relation $\delta\mathbf{A}$ is eliminated in equation (34) by using equation (33) and neglecting terms of $\delta n(k \pm 2k_0, w \pm 2w_0)$ as nonresonant:

$$\omega^2 - {\omega_{pe}}^2 = \frac{{\omega_{pe}}^2 k^2 {v_{os}}^2}{4}\left[\frac{1}{D(k + k_0, \omega + \omega_0)} + \frac{1}{D(k - k_0, \omega - \omega_0)}\right], \tag{35}$$

where $D(k, \omega) = \omega^2 - k^2c^2 - {\omega_{pe}}^2$ and the oscillation velocity $v_{os} = e^2{\mathbf{A}_0}^2/m^2c^2$. If back- and sidescatter are neglected as nonresonant the growth rate is determined as:

$$(\omega^2 - {\omega_{pe}}^2)\left[(\omega - \omega_0)^2 - (k - k_0)^2c^2 - {\omega_{pe}}^2\right] = \frac{{\omega_{pe}}^2 k^2 {v_{os}}^2}{4}. \tag{36}$$

The fastest growth occurs if the scattered light is resonant i.e.

$$(\omega - \omega_0)^2 - (k - k_0)^2c^2 - {\omega_{pe}}^2 = 0. \tag{37}$$

For $\omega = \omega_{pe} + \delta\omega$ with $\delta\omega \ll \omega_{pe}$ and a resonant scattered wave, using $(\omega - \omega_0)^2 = (\omega_{pe} + \delta\omega - \omega_0)^2 = (\omega_{pe} - \omega_0)^2 + 2\delta\omega(\omega_{pe} - \omega_0) + \delta\omega^2$, whereas $\delta\omega^2$ is neglectible, leads to:

$$(\omega^2 - {\omega_{pe}}^2) \cdot 2\delta\omega(\omega_{pe} - \omega_0) = \frac{{\omega_{pe}}^2 k^2 {v_{os}}^2}{4}, \tag{38}$$

therefore:

$$\delta\omega^2 = -\frac{\omega_{pe} k^2 {v_{os}}^2}{16(\omega_{pe} - \omega_0)}, \tag{39}$$

$$\delta\omega = \pm i\frac{k v_{os}}{4}\left(\frac{\omega_{pe}}{\omega_{pe} - \omega_0}\right)^{\frac{1}{2}} = i\Gamma, \tag{40}$$

where Γ is the growth rate. The last result is true because $\omega_0 > \omega_{pe}$. The wavenumber k is determined by equation (37)

$$k = k_0 + \frac{\omega_0}{c}\left(1 - \frac{2\omega_{pe}}{\omega_0}\right)^{\frac{1}{2}}. \tag{41}$$

2.3 Calculation of frequency mismatch in Raman scattering

To investigate the physics of Raman scattering the dispersion relation is used:

$$D_{\pm} = (\omega \pm \omega_0)^2 - (k \pm k_0)^2 c^2 - {\omega_{pe}}^2 = 0. \tag{42}$$

In case of FRS the wavenumber is $k = k_p \ll k_0$ and in case of BRS $k = 2k_0$. Therefore it is obvious that in FRS both modes, Stokes and anti-Stokes mode can occur. In case of BRS only Stokes mode occurs due to $(\omega + \omega_0)^2 - (3k_0)^2 c^2 - {\omega_{pe}}^2$ is inharmonic. Taking a look at FRS it becomes clear that there has to be a frequency mismatch between Stokes and anti-Stokes mode. Because Stokes mode is the more likely event $D_- = 0$, $\omega = \omega_{pe}$ is assumed. Using the binomial formula leads to:

$${\omega_{pe}}^2 - k^2 c^2 = 2(\omega_{pe}\omega_0 - k k_0 c^2), \tag{43}$$

which leads to

$$D_+ = 2({\omega_{pe}}^2 - k^2 c^2) = 4(\omega_{pe}\omega_0 - k k_0 c^2). \tag{44}$$

The frequency mismatch $\Delta\omega$ can be calculated by subtracting the following expression from $\omega - \omega_0$

$$\omega + \omega_0 = \sqrt{D_+ + {\omega_{pe}}^2 + (k + k_0)^2 c^2}.$$

If this value is equal to zero there is no frequency mismatch. Using equation (42) the frequency mismatch can be calculated the following:

$$\begin{aligned} \Delta\omega &= (\omega_{pe} + \omega_0) - \sqrt{(\omega_0 + \omega_{pe})^2 + D_+} \\ &= (\omega_{pe} + \omega_0) - (\omega_{pe} + \omega_0)\sqrt{1 + \frac{D_+}{\omega_0 + \omega_{pe}}}, \end{aligned} \tag{45}$$

a series expansion of the root leads to:

$$\begin{aligned} &= (\omega_{pe} + \omega_0) - (\omega_{pe} + \omega_0)\left[1 + \frac{D_+}{\omega_0 + \omega_{pe}}\right] \\ &= -\frac{1}{2(\omega_0 + \omega_{pe})} \\ &= -\frac{1}{2\omega_0}\left(1 + \frac{\omega_{pe}}{\omega_0}\right)^{-1} D_+. \end{aligned}$$

Now series expansion of the term in the brackets gives:

$$\begin{aligned} &= -\frac{1}{2\omega_0}\left(1 - \frac{\omega_{pe}}{\omega_0}\right) D_+ \\ &= -\frac{1 - \frac{\omega_{pe}}{\omega_0}}{\omega_0}({\omega_{pe}}^2 - k^2 c^2). \end{aligned}$$

With further expansions, replacement and reexpressing the terms the final result is:

$$\Delta\omega = -\frac{{\omega_{pe}}^2}{{\omega_0}^2} + \frac{9}{4}\frac{\omega_{pe}^4}{\omega_0^3}. \tag{46}$$

This is smaller than the growth rate, so the assumption of little perturbations is correct. If the frequency mismatch is to big only one mode of FRS would occur. Most likely Stokes mode would occur because it is the energetic favourable mode.

2.4 Dispersion relation of instabilities in the relativistic regime, growth rate of the Raman instabilities

To investigate what happens to short and ultra intense laser pulses in a plasma it is necessary to take relativistic effects into account. It is assumed that the pump laser propagates in the x-direction. The quantities for the density and the electro-magnetic potential are defined as:

$$n = \frac{n_e}{n_0}, \mathbf{a} = \frac{e\mathbf{A}}{mc^2},$$

where n_e is the electron density, n_0 is the background of ion density and $\mathbf{A}$ is the strength of the vector potential. The electric potential transforms into $\Phi \rightarrow e\Phi/mc^2$ and the momentum is defined as $p = \gamma u$. Some equations have to be redefined in the relativistic regime:

$$\left(\frac{\partial^2}{\partial t^2} - c^2\frac{\partial^2}{\partial x^2} + {\omega_{pe}}^2\frac{n}{\gamma}\right) a = 0 \tag{47}$$

$$\frac{\partial \mathbf{p}}{\partial t} + cu\frac{\partial p}{\partial x} = \frac{\partial \Phi}{\partial x} - \frac{1}{2\gamma}\frac{\partial}{\partial x}\mathbf{a}^2 \tag{48}$$

$$\frac{\partial n}{\partial t} + c\frac{\partial}{\partial x}\left(\frac{np}{\gamma}\right) = 0 \tag{49}$$

$$\frac{\partial^2}{\partial x^2}\Phi = {k_p}^2(n-1) \tag{50}$$

$$\gamma = (1 + p^2 + \mathbf{a}^2)^{\frac{1}{2}}. \tag{51}$$

Now little perturbations are assumed and the quantities are linearised ($u = \tilde{u} \rightarrow p = \tilde{p}$ and $u_0 = p_0 = 0, n = 1 + \tilde{n}, \mathbf{a} = \mathbf{a}_0 + \tilde{\mathbf{a}}$ and $\gamma_0 = (1 + {\mathbf{a}_0}^2)^{1/2}$). Fourier analysis leads to:

$$\left(\frac{\partial^2}{\partial t^2} - c^2\frac{\partial^2}{\partial x^2} + \frac{\omega_{pe}}{\gamma_0}\right)\mathbf{a}_0 = 0, \tag{52}$$

which gives, taking a wavelike ansatz, to the usual dispersion relation:

$${\omega_0}^2 = c^2{k_0}^2 + \omega_{pe}'^2. \tag{53}$$

$\omega_{pe}'^2 = {\omega_{pe}}^2/\gamma_0$ determines the effective plasma wave frequency. For easier reading ω_p instead of ω_{pe}' is written. The next order equation gives:

$$\left(\frac{\partial^2}{\partial t^2} - c^2\frac{\partial^2}{\partial x^2} + {\omega_p}^2\right)\tilde{\mathbf{a}} = -{\omega_p}^2\tilde{n}\mathbf{a}_0 + \frac{{\omega_p}^2}{{\gamma_0}^2}(\mathbf{a}_0\tilde{\mathbf{a}})\mathbf{a}_0. \tag{54}$$

This equation is the description of FRS. If now equation (51) is evolved, assuming $\tilde{p}, \tilde{\mathbf{a}} \ll \mathbf{a}_0$, the following result can be found:

$$\gamma^{-1} \simeq \gamma_0^{-1} - \frac{\mathbf{a}_0\tilde{\mathbf{a}}}{\gamma_0^3}. \tag{55}$$

With regards to the ponderomotive force, comprising a beat term $(1/2\ \partial\mathbf{a}^2/\partial x)$ between pump and scattered electro-magnetic wave leads for the first order momentum equation to:

$$\frac{1}{c}\frac{\partial}{\partial t}u = \frac{1}{\gamma_0}\frac{\partial}{\partial x}\tilde{\Phi} - \frac{1}{{\gamma_0}^2}\frac{\partial}{\partial x}(\mathbf{a}_0\tilde{\mathbf{a}}). \tag{56}$$

Taking a time derivative and substituting into equation (47) gives:

$$\left(\frac{\partial^2}{\partial t^2} + {\omega_p}^2\right)\tilde{n} = \frac{c^2}{{\gamma_0}^2}\frac{\partial^2}{\partial x^2}(\mathbf{a}_0\tilde{\mathbf{a}}), \tag{57}$$

describing the BRS.

Using the procedure of separating the quantities of equation (54) and (57) into a product of slowly varying envelope and a fastly variying phase yields:

$$\tilde{n} = \frac{n_1}{2}e^{-i\varphi} + \text{ c.c.} \tag{58}$$

$$\tilde{\mathbf{a}} = \left(\frac{\mathbf{a}_+}{2}e^{i\varphi_+} + \frac{\mathbf{a}_-}{2}e^{i\varphi_-}\right) + \text{c.c.} \tag{59}$$

$$\mathbf{a}_0 = \frac{\mathbf{a}_0}{2}e^{i\varphi_0} + \text{c.c. ,} \tag{60}$$

where φ is the scattered wave and φ_0 is the pump wave. The connection between φ_0 and φ is:

$$\varphi = kx - \omega t, \varphi_0 = k_0 x - \omega_0 t, \varphi_\pm = (k \pm k_0)x - (\omega \pm \omega_0)t. \tag{61}$$

The different matchings can be seen for the FRS, first the anti-Stokes (k_+) and secondly the Stokes mode (k_-) with a difference of k:

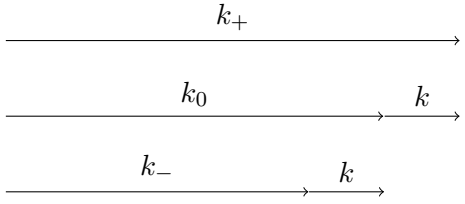

As explained before (2.3) only Stokes mode exists for BRS:

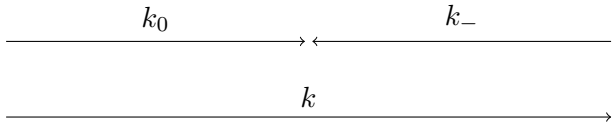

If only low frequency terms with $\varphi = \varphi_+ - \varphi_0 = \varphi_- + \varphi_0$ are taken into account, it can be seen that only terms with $\mathbf{a}_+\mathbf{a}_0^*$ and $\mathbf{a}_-\mathbf{a}_0$ will rise on RHS of equation (57). This leads to

$$(-\omega^2 + {\omega_p}^2)\frac{n_1}{2} = -\frac{c^2k^2}{4{\gamma_0}^2}(\mathbf{a}_+\mathbf{a}_0^* + \mathbf{a}_-\mathbf{a}_0). \tag{62}$$

If now D_e is defined as:

$$D_e = -\omega^2 + {\omega_p}^2, \tag{63}$$

equation (62) can be expressed as:

$$n_1(\omega, k) = -\frac{c^2k^2}{2{\gamma_0}^2 D_e}(\mathbf{a}_+\mathbf{a}_0^* + \mathbf{a}_-\mathbf{a}_0). \tag{64}$$

This equation can be used to identify the driving current on RHS of equation (54). Taking care of the polarisation of the pump wave vector:

$$\boldsymbol{a}_0 = \frac{\mathbf{a}_0}{2}\sigma e^{i\varphi_0} + \text{c.c.}, \tag{65}$$

with

$$\sigma = \begin{cases} \boldsymbol{e_y} \\ \frac{1}{\sqrt{2}}(\boldsymbol{e_y} + i\boldsymbol{e_z}) \end{cases}. \tag{66}$$

The first case represents the linear and the second the circular polarized light. This can be used to calculate ${\mathbf{a}_0}^2$:

$${\mathbf{a}_0}^2 = \mathbf{a}_0 \cdot \mathbf{a}_0 = (\frac{1}{2}a_0\sigma e^{i\varphi_0} + \frac{1}{2}a_0^*\sigma^* e^{-i\varphi_0})^2 \tag{67}$$

$$= \begin{cases} \frac{1}{4}{a_0}^2 e^{i2\varphi_0} + \frac{1}{2}|a_0|^2 \frac{1}{4}{a_0^*}^2 e^{i2\varphi_0} \\ \frac{1}{2}|a_0|^2 \end{cases}. \tag{68}$$

From this result the focus should be set on the circular polarized light because it is independent from the phase. Therefore the relativistic factor can be calculated via:

$$\gamma_0 = \sqrt{1 + {\mathbf{a}_0}^2} = \sqrt{1 + \frac{|a_0|^2}{2}}. \tag{69}$$

Calculating the nonlinear current (RHS of equation (54)) for $\varphi_\pm = \varphi \pm \varphi_0$ results in:

$$J(\omega - \omega_0) = \frac{{\omega_p}^2}{8{\gamma_0}^2}\left(\frac{c^2k^2}{D_e} + 1\right)\left(|a_0|^2 a_- + {a_0^*}^2 a_+\right) \tag{70}$$

$$J(\omega + \omega_0) = \frac{{\omega_p}^2}{8{\gamma_0}^2}\left(\frac{c^2k^2}{D_e} + 1\right)\left(|a_0|^2 a_+ + {a_0^*}^2 a_-\right). \tag{71}$$

Taking the LHS of equation (54) and defining:

$$D_{\pm} = -{\omega_{\pm}}^2 + {k_{\pm}}^2 c^2 + {\omega_{pe}}^2 = -\omega^2 + k^2 c^2 \pm 2(k k_0 c^2 - \omega_0 \omega) \tag{72}$$

yields

$$D_- a_- = 2 \cdot J(\omega - \omega_0) \tag{73}$$

$$D_+ a_+ = 2 \cdot J(\omega + \omega_0). \tag{74}$$

By multiplying equation (73) with a_0 and equation (74) with a_0^* the dispersion relation is determined as:

$$1 = \frac{{\omega_p}^2 |a_0|^2}{4\gamma_0} \left(\frac{c^2 k^2}{D_e} + 1 \right) \left(\frac{1}{D_+} + \frac{1}{D_-} \right). \tag{75}$$

From this equation the growth rate can easily be determined assuming $\omega = \omega_p + i\Gamma$, $\Gamma \ll \omega_p \ll \omega_0$. Starting at equation (73) and combining it with $D_{\pm} \simeq -2i\Gamma(\omega_p \pm \omega_0)$ as well as $D_e \simeq -2i\omega_p \Gamma$, where $c^2 {k_{max}}^2 = {\omega_p}^2$. Applying algebraic transformations the growth rate of FRS is determined by:

$$\Gamma_{FRS} = \frac{{\omega_p}^2 a_0}{\sqrt{8}\omega_0 \left(1 + \frac{{a_0}^2}{2}\right)}. \tag{76}$$

Taking a look at the non-relativistic limit $a_0 \ll 1$ it becomes clear that $\Gamma = {\omega_p}^2 / \sqrt{8}\omega_0 a_0$ and for the ultra-relativistic limit it is obtained $\Gamma \simeq {\omega_p}^2 / \sqrt{2}\omega_0 a_0 \sim a_0^{-1}$. For the BRS it is assumed $a_0 \gg \sqrt{\omega_p / \omega_0}$ and $\Gamma \gg \omega_p$. The upshifted wave is neglected as non-resonant this leads to:

$$D_- = \frac{{\omega_p}^2 {a_0}^2}{4{\gamma_0}^2} \left(\frac{c^2 k^2}{D_e} + 1 \right). \tag{77}$$

The maximum growth occurs for $k = k_0 + \omega_0 \sqrt{1 - 2\omega_p \omega_0}/c \simeq 2k_0$. In this case is the growth rate of BRS becomes:

$$\Gamma_{BRS} = \frac{\sqrt{3}}{2} \left(\frac{\omega_0}{2\omega_p} \right)^{\frac{1}{3}} \frac{a_0^{\frac{2}{3}}}{\sqrt{1 + \frac{{a_0}^2}{2}}} \omega_p. \tag{78}$$

The maximum growth occurs for $a_0 = 2$. This leads to $\Gamma \sim a_0^{-1/3}$ for $a_0 \gg 1$.

2.5 Parametric instabilities in the ultra-relativistic regime, influence of the radiation reaction force

The equation of motion for an electron moving in a given electro-magnetic field is still unsolved, despite first attempts to solve it started more than 100 years ago. It is well known that an accelerating electron emits radiation. The faster the electron moves, the more energy it is emitting. This energy can be substantial if the motion of an electron is ultra-relativistiv. Hence, taking only the Lorentz-force on the RHS of the equation of motion into account, this loss of energy cannot be accounted for and leads to incorrect

results of the electron energy computation. This problem of accouting the radiation loss is inherently quantum mechanical in nature [10]. However, in classical regime, the Landau-Lifshitz description of the radiation reaction force can be used [9]. In this thesis only the leading-order term of it will be taken into account, the terms of higher order are smaller in magnitude and can be neglected in a first approximation.

The assumptions about the plasma and laser made in the beginning (section 2.1) are still valid. For conformity reasons and better calculations the propagation of a circularly polarized pump laser in the plasma is considered. The following equation can be easily derived from the Vlasov equation (1). The leading order term of the Landau-Lifshitz radiation reaction force is included:

$$\frac{\partial \mathbf{p}}{\partial t} + \mathbf{v}\nabla\mathbf{p} = -e\left(\mathbf{E} + \frac{1}{c}(\mathbf{v}\times\mathbf{B})\right) - \frac{2e^4}{3{m_e}^2c^5}\gamma^2\mathbf{v}\times\left[\left(\mathbf{E} + \frac{1}{c}(\mathbf{v}\times\mathbf{B})\right)^2 - \left(\frac{\mathbf{v}}{c}\mathbf{E}\right)^2\right]. \quad (79)$$

The radiation reaction term is ignored first and the equation of motion for the transverse momentum and the time derivative of the transverse velocity solved. The electromagnetic fields are written again in expressions of the potentials (section 2.2).

$$\mathbf{p}_\perp = \frac{e}{c}\mathbf{A} \quad (80)$$

$$\frac{\partial \mathbf{v}}{\partial t} = \frac{e\nabla\Phi}{m_e\gamma_0} - \frac{e^2}{2{m_e}^2{\gamma_0}^2c^2}\nabla|\mathbf{A}|^2. \quad (81)$$

The scattering of the laser leads to a total vector potential of:

$$\mathbf{A} = \frac{1}{2}\left[A_0 e^{i\varphi_0} + \delta A_+ e^{i\mathbf{k}_t\mathbf{x}_t}e^{i\varphi_+} + \delta A_-^* e^{-i\mathbf{k}_t\mathbf{x}_t}e^{-i\varphi_+}\right] + \text{c.c.}, \quad (82)$$

which gives the plasma oszillations:

$$\delta\tilde{n} = \frac{e^2k^2}{2{m_e}^2{\gamma_0}^2c^2D_e}(A_0^*\delta A_+ + A_0\delta A_-), \quad (83)$$

with $D_e = \omega^2 - \omega_p'2$, $\delta n/n_0 = (\delta\tilde{n}/2)e^{i\varphi}e^{i\mathbf{k}_t\mathbf{x}_t} + \text{c.c.}$ and $\varphi = \varphi_+ - \varphi_0 = \varphi_- + \varphi_0$. This equation causes an axial component of velocity and momentum. The radiation reaction term is proportional to:

$$\left(\mathbf{E} + \frac{1}{c}(\mathbf{v}\times\mathbf{B})\right)^2 - \left(\frac{\mathbf{v}}{c}\mathbf{E}\right)^2, \quad (84)$$

which is, written in terms of potentials, equal to:

$$= \left[-\frac{1}{c}\frac{\partial\mathbf{A}}{\partial t} - \nabla\Phi + \frac{1}{c}\left(\mathbf{v}\times(\nabla\times\mathbf{A})\right)\right]^2 - \left[\frac{\mathbf{v}}{c}\left(-\frac{1}{c}\frac{\partial\mathbf{A}}{\partial t} - \nabla\Phi\right)\right]^2. \quad (85)$$

Using a standard vector identity to transform the doubled vector product yields:

$$= \left[-\frac{1}{c}\frac{\partial\mathbf{A}}{\partial t} - \left(\frac{\mathbf{v}}{c}\nabla\right)\mathbf{A} - \nabla\Phi + \frac{1}{c}\left((\nabla\mathbf{A})\mathbf{v}\right)\right]^2 - \left[\frac{\mathbf{v}}{c^2}\frac{\partial\mathbf{A}}{\partial t} + \frac{\mathbf{v}}{c^2}\nabla\Phi\right]^2. \quad (86)$$

Now using a linear approximation, i.e. ignoring $\nabla\varphi$ and $\mathbf{v}\nabla\varphi$ terms, the radiation reaction term becomes:

$$\simeq \left[-\frac{1}{c}\frac{\partial \mathbf{A}}{\partial t} - \left(\frac{\mathbf{v}}{c}\nabla\right)\mathbf{A}\right]^2 + \left[\frac{1}{c}(\nabla\mathbf{A})\mathbf{v})\right]^2 - \left[\frac{\mathbf{v}}{c^2}\frac{\partial \mathbf{A}}{\partial t}\right]^2. \tag{87}$$

Taking $\mathbf{A} = \mathbf{A}_t e^{-i\varphi_0}$ with the usual definition $\varphi_0 = k_0 x - \omega_0 t$ leads to

$$\frac{\partial \mathbf{A}}{\partial t} = -i\omega_0\mathbf{A} \text{ and } \nabla\mathbf{A} = ik_0\mathbf{A}. \tag{88}$$

This now can be substituted into the radiation reaction term:

$$-\frac{2}{3}\frac{e^4}{m^2c^5}\gamma^2\mathbf{v}\left[\left(\frac{i\omega_0}{c}\mathbf{A} - \beta_z ik_0\mathbf{A}\right)^2 + \left(\frac{1}{c}ik_0\mathbf{v}_t\mathbf{A}\right)^2 - \left(\frac{\mathbf{v}_t}{c^2}i\omega_0\mathbf{A}_t\right)^2\right]. \tag{89}$$

It is known that:

$$k_0 = \frac{\omega_0}{c}\varepsilon_0 \text{ with } \varepsilon_0 = \sqrt{1 - \frac{{\omega_p}^2}{{\omega_0}^2}}. \tag{90}$$

By also ignoring the occuring ${\beta_z}^2$ (linear approximation) this result becomes:

$$-\frac{2}{3}\frac{e^4}{m^2c^5}\gamma^2\mathbf{v}\left[\mathbf{A}^2\left(1 - 2\beta_z + 4\beta_z\frac{{\omega'_p}^2}{{\omega_0}^2} - \frac{{\omega'_p}^2}{{\omega_0}^2}\frac{{v_t}^2}{c^2}\right)\right]. \tag{91}$$

Only the transversal velocity component is considered, as it is needed in the wave equation, so a perturbative approximation can be used:

$$\mathbf{p}_\perp = \frac{e}{c}\mathbf{A}_\perp \text{ and } \mathbf{v}_\perp = \frac{e}{mc\gamma}\mathbf{A}_\perp. \tag{92}$$

Since assuming ${\omega'_p}^2{\omega_0}^2 \ll 1$ and therefore ignoring the last two terms of equation (91) the transverse component of the momentum becomes:

$$\frac{\partial}{\partial t}\left(\mathbf{p}_\perp - \frac{e}{c}\mathbf{A}\right) = -\frac{\mu e\omega_0\gamma}{c}\mathbf{A}|\mathbf{A}|^2(1 - 2\beta_z), \tag{93}$$

where $\mu = 2e^4\omega_0/3m^3c^7$ and $p_\perp$ can be expresses the same way as equation (82). The procedure is again to split the momentum in a perpendicular and a $\mathbf{p}_0$ part. First all $e^{i\varphi_0}$ terms have to be collected:

$$\mathbf{p}_0 = \frac{e}{c}\mathbf{A}_0(1 - i\varepsilon a_0^2\gamma_0), \tag{94}$$

where $\varepsilon = r_e\omega_0/3c = 7.38\cdot10^{-9}$ with $r_e = e^2/mc^2$ the classical electron radius and a laser of wavelength $\lambda_0 \simeq 0.8\mu m$. Now focussing on the perpendicular part the remaining terms are collected, the equation is fourier analyzed and the result applied to equation (82). Rearranging the terms leads to:

$$\frac{c}{e}\mathbf{p}_\perp = \delta\mathbf{A}_+\left[1 - \frac{i\varepsilon a_0^2\omega_0\gamma_0}{\omega + \omega_0}\right] - \frac{i\varepsilon a_0^2\omega_0\gamma_0}{\omega + \omega_0}\left[\left(1 + \frac{a_0^2}{4\gamma_0^2}\right) - \frac{\omega}{kc}\frac{k^2c^2{a_0}^2}{2\gamma_0 D_e}\right](\delta\mathbf{A}_+ + \delta\mathbf{A}_-). \tag{95}$$

This leads to a wave equation for $e^{i\varphi_+}$ which is:

$$(\omega+\omega_0)^2 - {k_\perp}^2c^2 - (k+k_0)^2c^2 = \frac{\omega_p e^2}{\gamma_0}\mathbf{p}_\perp\left(\frac{c}{e}\right) + \omega_p e^2\frac{\mathbf{p}_0}{\gamma_{i\varphi}}\left(\frac{c}{e}\right) + \frac{\omega_p e^2}{\gamma_0}\frac{\delta n}{n_0}\mathbf{p}_0\left(\frac{c}{e}\right), \quad (96)$$

according to equation (83). Using the quantities which were just derived, rearranging, simplifying and ignoring the $k_\perp$ term the wave equation (98) for the anti-Stokes mode. The same calculations are followed for $\delta\mathbf{A}_-$ which is the Stokes mode:

$$D_\pm\delta\mathbf{A}_\pm = \frac{\omega_p {a_0}^2}{4{\gamma_0}^2}\left[\frac{k^2c^2}{D_e}\left(1 \mp i\varepsilon {a_0}^2\gamma_0 + \frac{2i\varepsilon {a_0}^2\gamma_0}{kc}\frac{\omega\omega_0}{\omega\pm\omega_0}\right)\right. \quad (97)$$

$$\left. - \left(1 + 4i\varepsilon\gamma_0^3\frac{\omega_0}{\omega\pm\omega_0}\right)\right](\delta\mathbf{A}_+ + \delta\mathbf{A}_-). \quad (98)$$

With following definition of $D_\pm$ and the definition of $R_\pm$ as:

$$D_\pm = (\omega\pm\omega_0)^2 - (k\pm k_0)^2c^2 - {\omega_p}^2\left(1 - i\varepsilon {a_0}^2\gamma_0\frac{\omega_0}{\omega\pm\omega_0}\right) \quad (99)$$

$$R_\pm = \frac{{\omega_p'}^2{a_0}^2}{4{\gamma_0}^2}\left[\frac{k^2c^2}{D_e}\left(1 \mp i\varepsilon {a_0}^2\gamma_0 + \frac{2i\varepsilon {a_0}^2\gamma_0}{kc}\frac{\omega\omega_0}{\omega\pm\omega_0}\right)\right.$$

$$\left. - \left(1 \mp i\varepsilon {a_0}^2\gamma_0\frac{\omega}{\omega\pm\omega_0} + 4i\varepsilon\gamma_0^3\frac{\omega_0}{\omega\pm\omega_0}\right)\right] \quad (100)$$

This leads to the dispersion relation:

$$\left(\frac{R_+}{D_+} + \frac{R_-}{D_-}\right) = 1 \quad (101)$$

The growth rate of FRS is:

$$\Gamma_{FRS} = -\frac{\omega_p e^2\varepsilon {a_0}^2}{2\omega_0} \pm \frac{{\omega_p}^2 a_0}{\sqrt{8}{\gamma_0}^2\omega_0}\cos(\theta/2) \times \sqrt[4]{(1+\varepsilon^2{a_0}^2\gamma_0^4)^2 + \varepsilon^2 a_0^4{\gamma_0}^2\left(\frac{\omega_0}{\omega_p}\right)} \quad (102)$$

$$\theta = \tan^{-1}\left(\frac{-\varepsilon {a_0}^2\gamma_0(\omega_0/\omega_p)}{1+2\varepsilon^2{a_0}^2\gamma_0^4}\right).$$

3 Numerical analysis of the dispersion relation

For comparison the plots including radiation reaction (RR) force effects are shown next to those which do not include radiation reaction effects. To obtain the results the dispersion relations were normalized by dividing with ω_0^6 respectively ω_0^8. This leads to a normalisation of k by k_0 using equation (90). The normalised plasma frequency ω_p is calculated via $\omega_p/\omega_0 = \sqrt{n_0/\gamma_0 n_c}$. If $n/\gamma_0 n_c > 1$ there will be no zeroth order propagation, because k_0 would become imaginary (equation (90)). The values fulfilling this conditions are marked in the plots. From now on the quantities represent the normalised quantities, e.g. k stands for k/k_0. The roots of the sixth order equation yields either four real and two complex conjugated solutions or six real solutions. In case of taking care of radiation reaction force eigth complex solutions are obtained. The imaginary part of the solutions implicates the growth rate. A negative growth rate indicates that the mode is damped, an imaginary part of order 10^{-8} or lower indicates a stable solution, and a positive imaginary part leads to a growth of the mode.

3.1 Growth rate and the related frequency for different parameters

First of all some specific solutions of the dispersion relation for different values of a_0 are plotted. The plots show the growth rate (solid line) and its related frequency (dashed line), which is the real part of this solution, versus a range of k. At low n/n_c and a_0 radiation reaction does not play any role (Figs. 1 and 2). The position as well as the magnitude of the unstable branches are the same. Radiation reaction leads to longer edges of the unstable branches, because the damping term leads to a continuous evolution in the k-space.

The different branches can be easily identified in both pictures. The branch on the left, in the low k-value regime, belongs to the modulational instabilities. The second branch is the Stokes mode of FRS. The beginning of the third branch is the anti-Stokes mode of FRS and at $k \approx 2$ the instability of BRS is placed. If the parameters change, the branches can broad and at some points merge [6] and can be also seen in Fig. 9. To investigate the influence of radiation reaction effects on this merging and broadening the laser amplitude is raised to $a_0 > 10$.

Rising the laser amplitude up to $a_0 = 20$ leads to interesting effects (Fig. 3 and 4). In the case without RR force the two first branches narrow and the third branch broadens up but there is no merging of the branches. Including RR leads to a merging of the two Raman branches and a new branch occurs near to $k = 1$, which is close to laser mode. This case, where a new branch emerges, has not been taken into account before. The merging of the branches leads to a larger scale of k vectors which could excite an instability. So it has to be taken into account that in this region also instabilities will occur.

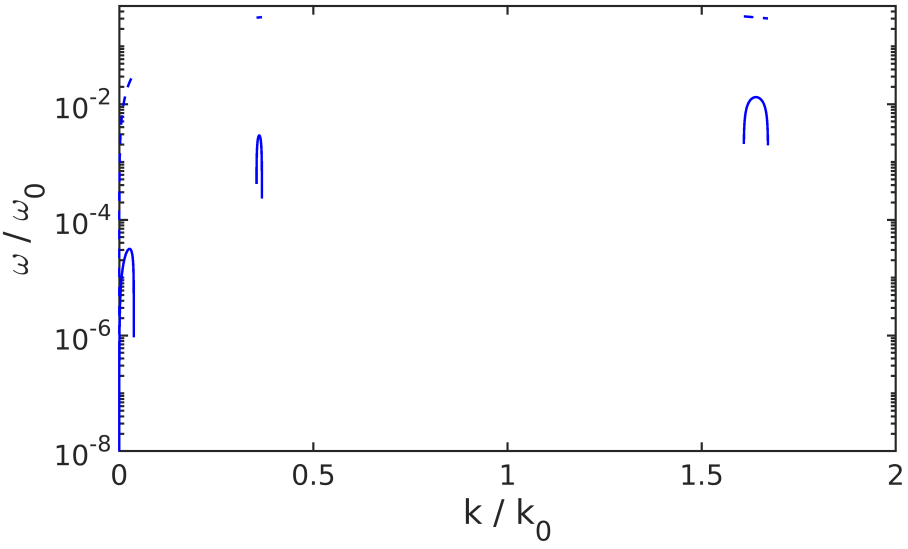

Fig. 1: Growth rate and its related frequency at $n/n_c = 0.1$ and $a_0 = 0.05$ without RR force

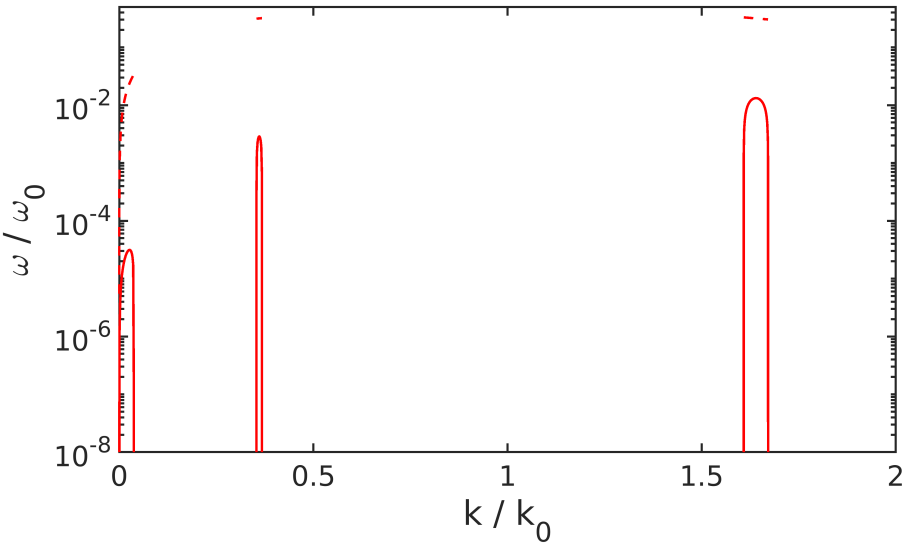

Fig. 2: Growth rate and its related frequency at $n/n_c = 0.1$ and $a_0 = 0.05$ including RR force

If the laser amplitude is raised further to $a_0 = 40$, a completely new phenomena can be seen. Comparing the two results (Figs. 5 and 6) it can be seen, that they both contain a nearly similar big branch.

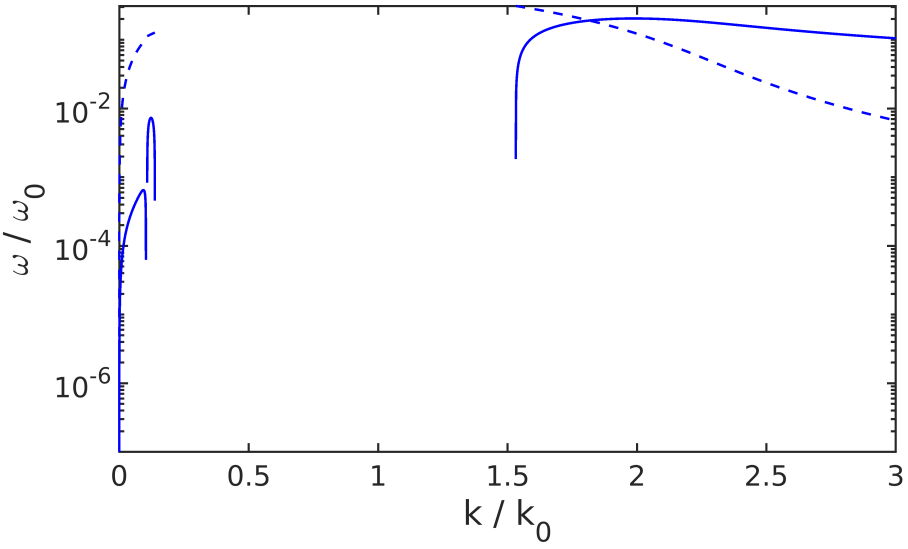

Fig. 3: Growth rate and its related frequency at $n/n_c = 0.2$ and $a_0 = 20$ without RR force

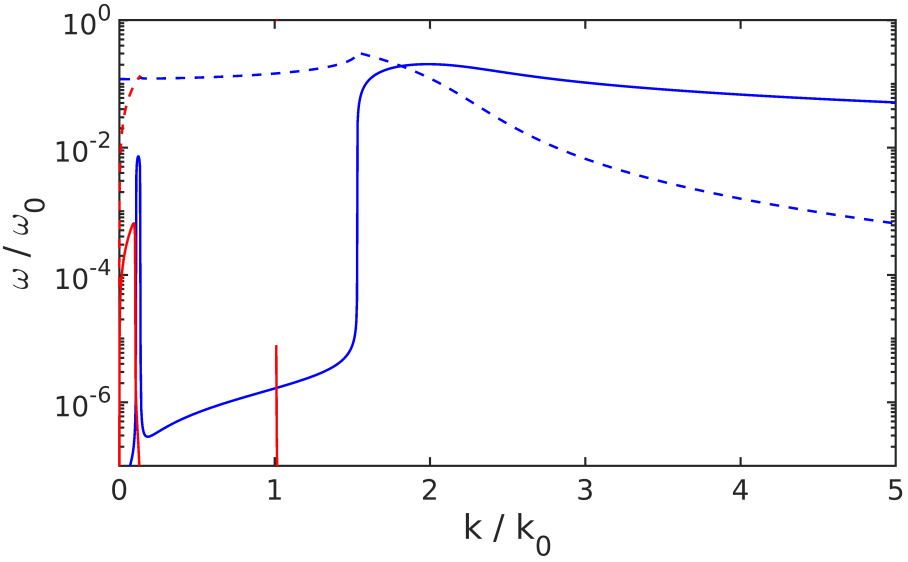

Fig. 4: Growth rate and its related frequency at $n/n_c = 0.2$ and $a_0 = 20$ including RR force

In the case of radiation reaction force the so-called quasi-modes occur, plotted by the blue lines. Those modes are fixed to a specific range of k but their magnitude is quite smaller than the magnitude of the other modes which exists at the same k value. Due

to this mismatch of the magnitudes only the dominant mode will be the driving one for the instability.

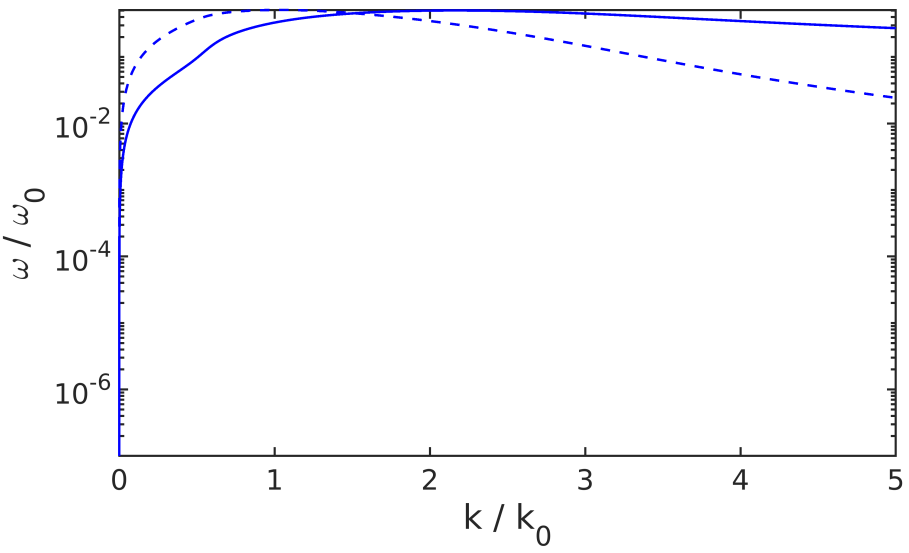

Fig. 5: Growth rate and its related frequency at $n/n_c = 10$ and $a_0 = 40$ without RR force

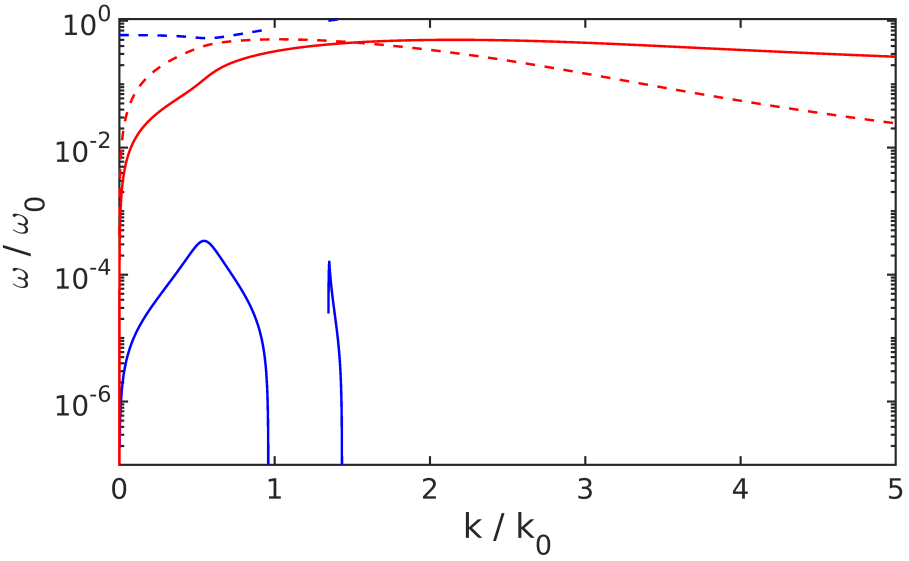

Fig. 6: Growth rate and its related frequency at $n/n_c = 10$ and $a_0 = 40$ including RR force. Quasi-modes represented by the blue line

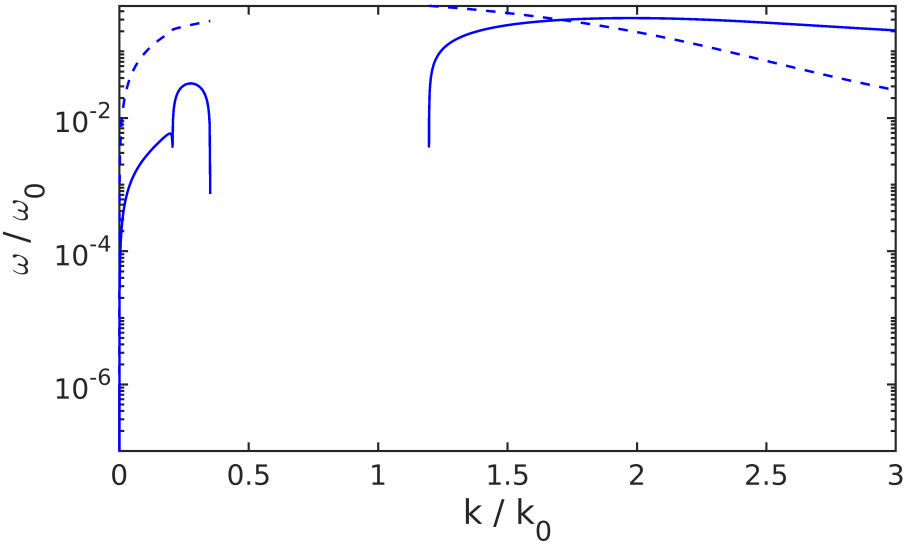

Fig. 7: Growth rate and its related frequency at $n/n_c = 10$ and $a_0 = 250$ without RR force

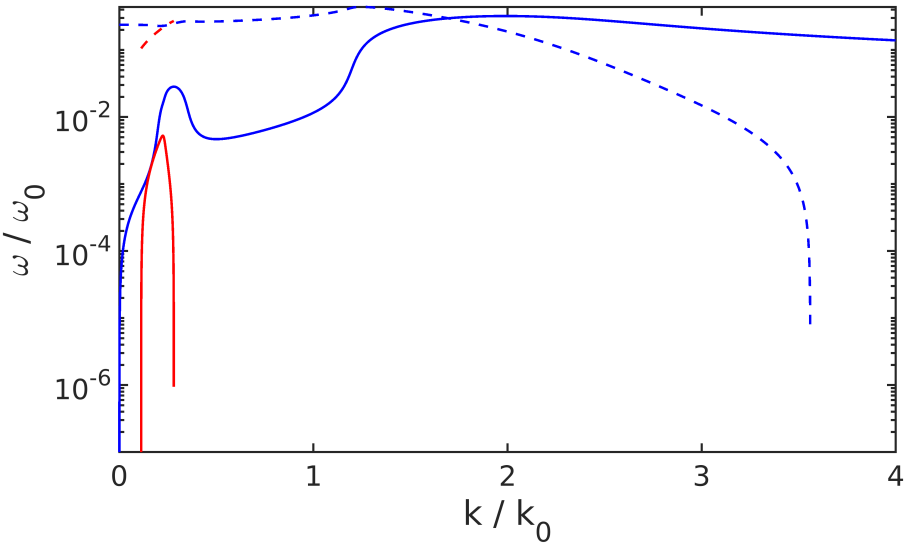

Fig. 8: Growth rate and its related frequency at $n/n_c = 10$ and $a_0 = 250$ including RR force, quasi-mode plotted in red line

Increasing the laser amplitude of the pump laser up to $a_0 = 250$, again a quasi mode occurs, shown by the red line. Including radiation reaction force leads to a merging of all unstable branches. If the density of the plasma is decreased the quasi-mode will move

to lower k and become a modulational instability. The merging of the branches leads to an enhancement of the growth rate, especially for FRS.

3.2 Parameters map for the number of unstable branches

As could be seen in the section before, the number of unstable branches depends on the density n/n_c and laser amplitude a_0. To see an overall behaviour of the plasma instabilities the number of different unstable branches are plotted with plasma density and laser amplitude.

The results can be seen in Fig. 9 without RR force and in Fig. 10 with RR force. For the purpose of identifying a branch a limit for the growth rate to exceeds 10^{-6} is set. This threshold is choosen because imaginary parts below this value can be assumed not to have any effects on the plasma. Two branches are distinguished as different if the imaginary part of this solution falls below 10^{-8}. These two thresholds cause the spiky area in the upper middle of Fig. 10, as well as to the blue part in the upper left corner, because certain modes in this region do not exceed this threshold.

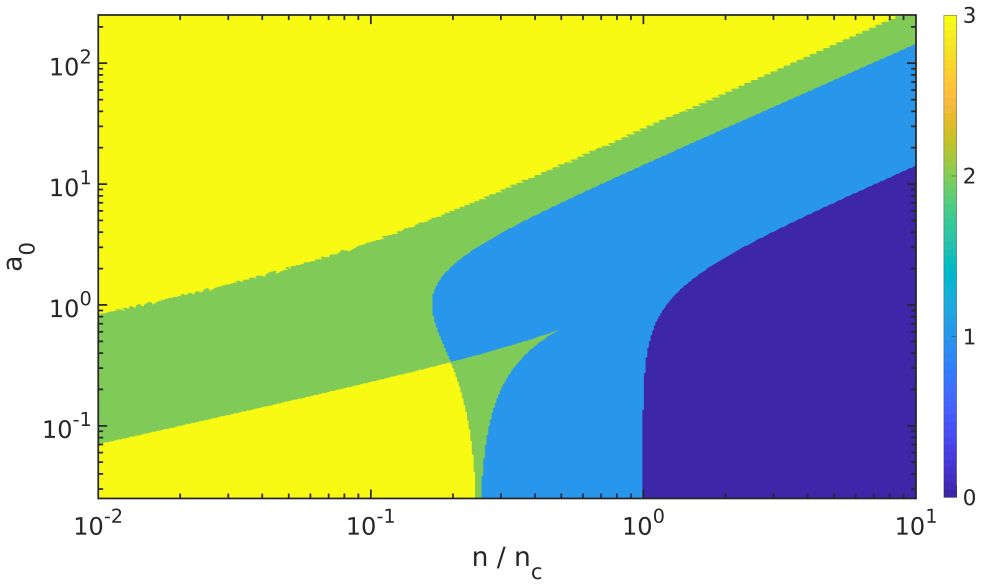

Fig. 9: Number of unstable branches without RR force. The colorbar indicates the number of unstable branches.

In Fig. 9 five different domains are existing. The sixth one, the dark blue, is the region of no zeroth order laser propagation. Of course this domain, as well as the low a_0 domains stay the same in case of radiation reaction (Figs. 10 and 2). The merging of the Raman branches at low density starts at $a_0 \leq 1$, depending on the density.
On the right side of Fig. 10 in the lower green area one quasi mode exists below a big branch. This quasi mode splits into two quasi modes if a_0 is increased (Fig. 6). The result

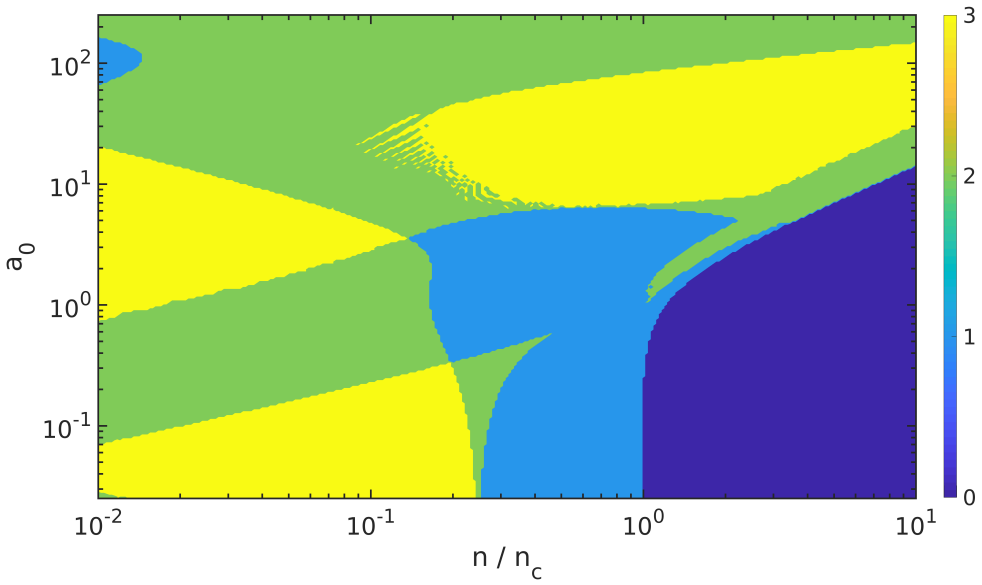

Fig. 10: Number of unstable branches including RR force. The colorbar indicates the number of unstable branches.

of the area of highest a_0 and n/n_c is shown in Fig. 8. If the laser amplitude stays at the same level and the density is decreased, this spike moves quickly near to $k \approx 10^{-1}$. If the n/n_c is unchanged and the a_0 is decreased, this quasi mode becomes again a single mode, the modulational instability (Fig. 4).

3.3 Maximum growth rate

Figs. 11 and 12 show the maximum growth rate which is excited with respect to a_0 and n/n_c. It is important that this growth rate is not determined at a fixed k. It is the maximum value occuring in the numerical solution. For easier comparison the log10 of the growth rate is plotted. Because of this logarithmic plotting, the down right corner, which is the area of no zeroth-order propagation, stays white. It corresponds to the same blue in Figs. 9 and 10.

It can be seen that the maximum of the growth rate stays more or less the same in Figs. 11 and 12. The growth rate including radiation reaction effects is slightly higher, mostly in the region of high a_0 and $n/n_c \approx 10^{-1}$. This is in accordance with the results of Kumar et al. [7]. Without radiation reaction force the total maximum of the growth rate is ≈ 0.57 which matches well with Ref. [6].

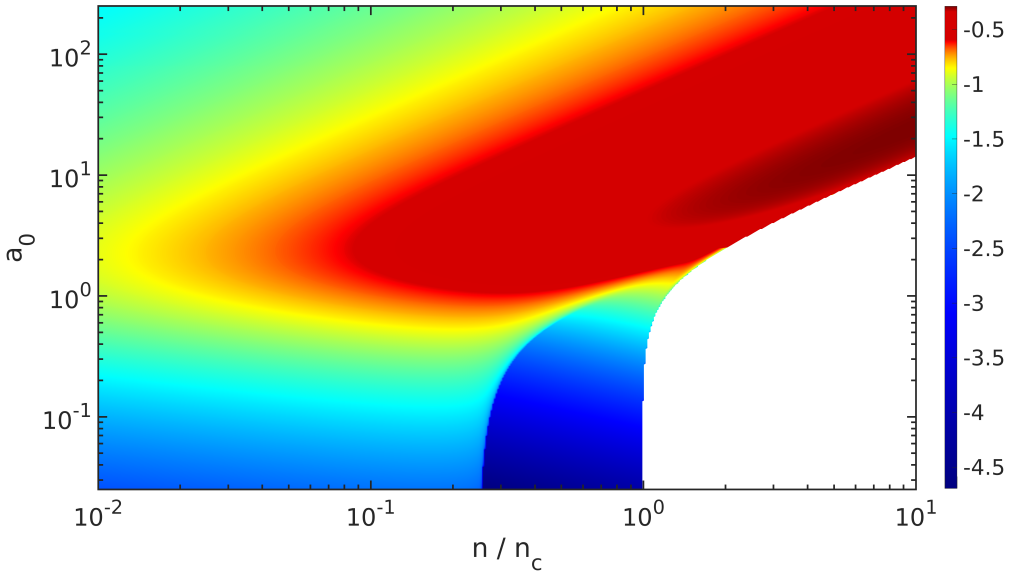

Fig. 11: Maximum growth rate without RR force

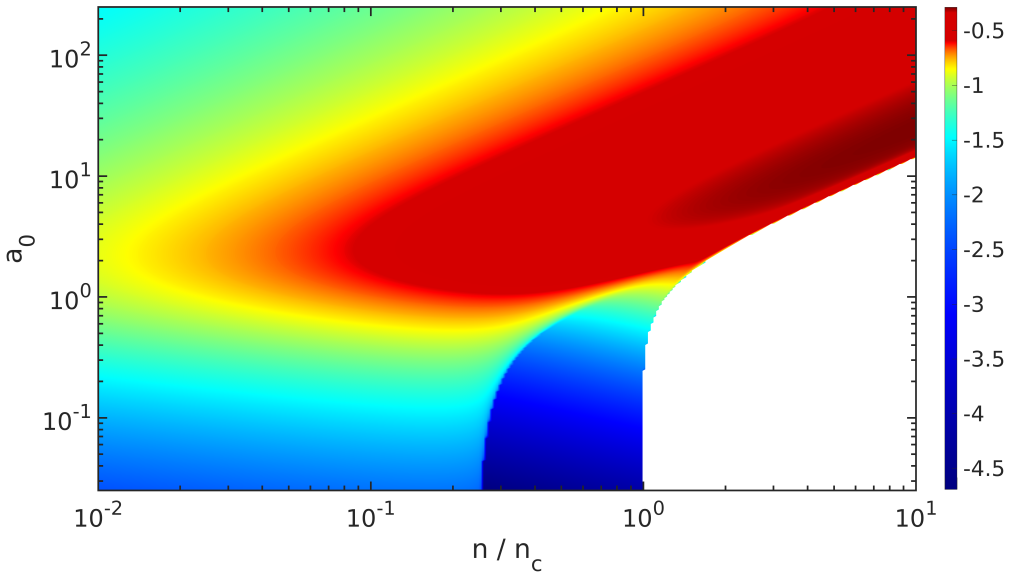

Fig. 12: Maximum growth rate including RR force

3.4 Maximum k value of an instability

The last quantity compared in the analysis part is the maximum k value, at which an instability can be excited. The maximum k value is again plotted using a log10 scale (see Figs. 13 and 14).

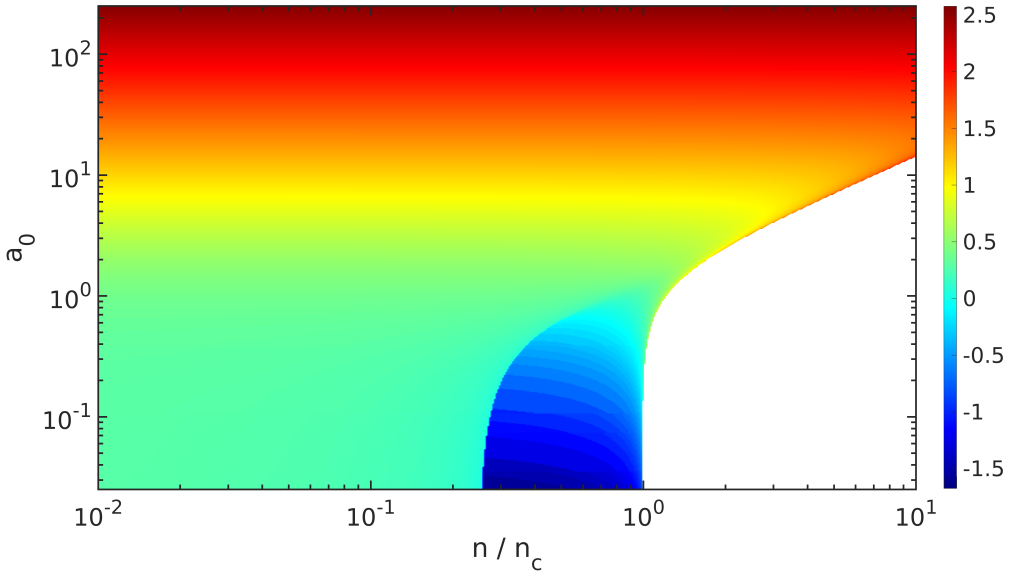

Fig. 13: Maximum k value without RR force

In the low a_0 regime the plots are more or less the same, as expected. At low density and laser amplitude the maximum k value which excites an instablity is nearby $k = 2$ which is identified as BRS. This maximum value grows rapidely in the relativistic and ultra-relativistic regime. In case of no radiation reaction this growth is limited to $k = 355$. On including the radiation reaction force the maximum k value for which an instability is escited becomes higher. The upper limit is set to $k = 500$. If the maximum k gets higher, the possible wavelength $\lambda = 2\pi/k$ becomes smaller. Due to this short wavelength perturbations the shape can be destroyed. This could be interesting if the shape of a laser pulse plays an important role.

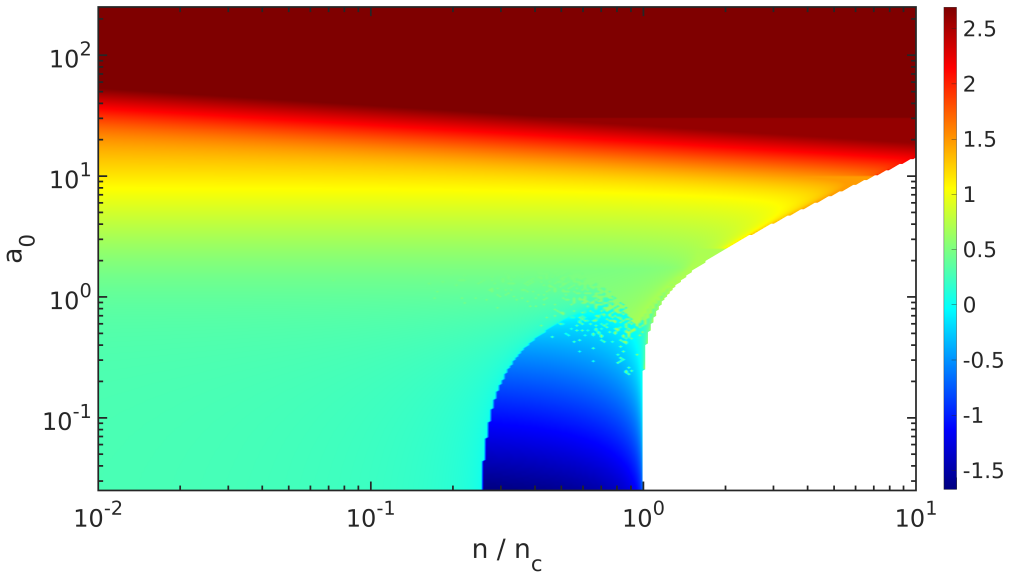

Fig. 14: Maximum k value including RR force

4 Conclusion of the results

The inclusion of the leading-order term of Landau-Lifshitz radiation reaction equation brings up new interesting effects. The most important fact is the merging of the two Raman branches (Fig. 4). This causes a larger unstable range, i.e. the parametric instabilities occur in a large range of wavelengths. The merging of the Raman branches can cause the growth rate to become higher, as different modes can easily overlay, which has effects on nearly every application of high-intensity laser-plasma interaction. Also the existence of new instabilities as in Fig. 4 and the excitation of quasi-modes indicates new physical phenomena. Those quasi-modes can be very important in multi-dimensional laser-plasma interaction.

Radiation reaction effects do not influence the overall maximum growth rate for a large range of parameters. But as it can be seen in section 3.2 the growth rate of FRS or the modulational instability can also be slightly increased at higher value of laser vector potential, where radiation reaction force effects are supposed to be strongest. Also the merging of the branches will lead to an enhancement of the growth rate.
Most of the previously mentioned effects by radiation reaction can also be seen in Fig. 10. Instead of five different unstable domains corresponding to instabilities, eight different domains are obtained, showing the impact of radiation reaction force clearly on the parametric instabilities. The exact implications of these unstable domains needs further investigation. It seems that the quasi modes arise mostly in the high density regime. There are some points where the modulational instability changes its position on the k axes and becomes a quasi mode. This point in between where the two branches overlap could also introduce some new effects.

In conclusion, the main effect of radiation reaction is the merging of the two Raman branches as well as excitation of new modes. The study of these modes and the effect of the merging open up the possibility for new effects in laser-plasma interaction.

5 Appendix

References

[1] Paul Gibbon. *Short Pulse Laser Interactions with Matter: An Introduction*. World Scientific Publication Company, 2005.

[2] U. Teubner and P. Gibbon. "High-order harmonics from laser-irradiated plasma surfaces". In: *Rev. Mod. Phys.* 81 (2 Apr. 2009), pp. 445–479. DOI: 10.1103/RevModPhys.81.445. URL: http://link.aps.org/doi/10.1103/RevModPhys.81.445.

[3] Wim Leemans and Eric Esarey. "Laser-driven plasma-wave electron accelerators". In: *Physics Today* 62.3 (2018/03/28 2009), pp. 44–49. DOI: 10.1063/1.3099645. URL: https://doi.org/10.1063/1.3099645.

[4] William Kruer. *The Physics Of Laser Plasma Interactions (Frontiers in Physics)*. Westview Press, 2003.

[5] Keith A. Brueckner and Siebe Jorna. "Laser-driven fusion". In: *Rev. Mod. Phys.* 46 (2 Apr. 1974), pp. 325–367. DOI: 10.1103/RevModPhys.46.325. URL: http://link.aps.org/doi/10.1103/RevModPhys.46.325.

[6] S. Guerin et al. "Modulational and Raman instabilities in the relativistic regime". In: *Physics of Plasmas* 2.7 (1995), pp. 2807–2814. DOI: 10.1063/1.871178. URL: http://link.aip.org/link/?PHP/2/2807/1.

[7] Naveen Kumar, Karen Z. Hatsagortsyan, and Christoph H. Keitel. "Radiation-Reaction-Force-Induced Nonlinear Mixing of Raman Sidebands of an Ultraintense Laser Pulse in a Plasma". In: *Phys. Rev. Lett.* 111 (10 Sept. 2013), p. 105001. DOI: 10.1103/PhysRevLett.111.105001. URL: https://link.aps.org/doi/10.1103/PhysRevLett.111.105001.

[8] *The Extreme Light Infrastructure Project*. URL: https://eli-laser.eu.

[9] L. D. Landau and E. M. Lifshitz. *The Classical Theory of Fields*. Fourth Revised English. Vol. 2. Course of Theoretical Physics. Butterworth-Heinemann, 2005.

[10] A. Di Piazza et al. "Extremely high-intensity laser interactions with fundamental quantum systems". In: *Rev. Mod. Phys.* 84 (3 Aug. 2012), pp. 1177–1228. DOI: 10.1103/RevModPhys.84.1177. URL: http://link.aps.org/doi/10.1103/RevModPhys.84.1177.

List of Figures

Development of MATLAB code for numerical solutions

This part of the thesis describes the development of MATLAB code for the numerical analysis of the dispersion relation in laser-plasma interaction. It is based on the code which was developed for the Projektpraktikum "Numerical solution of dispersion relation in laser-plasma interactions" carried out at MPIK Heidelberg.

The code consists mainly of three different parts: The header, the calculation of the dispersion relations roots and the sorting algorithm.

The header defines:

- The number of points investigated for each quantity
- The definition of the maximum k value investigated and the numer of different k steps
- For some applications it is useful to investigate the k range on a logarithmic scale. Also a linear scale could be used for other applications
- ε which could be set to be 0 to obtain the results without radiation reaction
- 'dense' and 'power' contain the values of a_0 and n/n_c investigated in the loop
- Empty arrays to improve the code performance

```
%------Header -----%

points = 250;
iterations = 10000;
kmax = 3;
khelp = kmax * logspace(-4,0,iterations);
k = khelp-khelp(1);
sorted = zeros([8 iterations]);
r = zeros([8 iterations]);
eps = 7.38*10^(-9);

J = [ 1; 2; 3; 4; 5; 6; 7; 8 ];
maxgrowth = zeros([points points]);
solofdisp = zeros([points points]);
dense = logspace(-2,1, points)';
power = 2.5*logspace(-1, 2, points);
```

The next part is embedded into two different loops, one for different density values as well as one for different intensity values. For each of this values the coefficients and quantities used in the calculation of dispersion relation are determined. To ensure only considering physical solutions the loop breaks if $\omega_p \geq 1$.

```
for l= 1:1:points
  for j = 1:1:points

%------Calculation of the parameters-----%

        a0= power(j);
        n = dense(l);
        y0 = sqrt( 1+ (a0^2) / 2);
        wp = sqrt ( n / y0 );
        e0 = sqrt(1 - wp^2);
        x = 1i *eps*a0.^2*y0;
        b = a0^2 / (4 * y0^2);
        c = 1i * 4 * eps * y0^3;

      if wp >= 1
         continue

      else

      [...]

      end
   end
end
```

If this condition is true, a new loop begins which calculated different values for k. For each value of k the polynomia p of dispersion relation is calculated via its coefficients (`C1-C6`), and its roots are stored in the array `r`. For some investigation e.g. the number of instable branches it could be useful to create the k value logspaced

```
%----Calculation of the polynomial dispersion relation and its solution ---%

% k = linspace(0, kmax, iterations) %only for variable kmax
for m=1:1:length(k);

%------Coefficients of dispersion relation polynomia -----%
C6 = -5 - 2 * e0^2 * k(m).^2 + (-1 + 2 * b) * wp^2;
    C5 = 8 * e0^2 * k(m) + 2 * wp^2 * (x + b * (c + 3 * x));
    C4 = 4 + e0^4 *k(m).^2 *(-4 + k(m).^2) + (5 - 2* b)* wp^2 - [...];
    C3 = -2 *(wp^2* (b* c *(-2 + wp^2) + 2 *b* wp^2 * x + [...];
    C2 = -4* b* e0* k(m)* wp^2* x + 2 *b *e0^3 *k(m).^3 [...];
    C1 = 2* wp^2 *(2* b *e0^3* k(m).^2* x - b *e0* k(m)* wp^2[...];
    C0 = -wp^2 * (wp^4 *x* (2* b* c + x) + e0^4* k(m).^2 [...];
```

```
p = [1 0 C6 C5 C4 C3 C2 C1 C0];
r(:, m) = roots(p);
```

As the roots command does not store the values belonging to each other in the same column of r one needs the next part, the sorting algorithm.
Having a look into the solutions given by the roots command the sorting algorithm is specified. The solution one obtains are, depending on the values of a_0 and n/n_c, for the low k regime:

- Two values with real part at $\approx \pm 2$, representing the Stokes respictively the Anti-Stokes mode
- Two values with real part at $\approx \pm 1$, which represent the pump laser mode
- Two values with real part at $\approx \pm \omega_p$ representing the plasma mode
- And two values with real part ≈ 0 which grow over the time

Mostly the real part of five of those modes is bigger than zero, in a few rare cases the roots give only four real parts bigger than zero.
For the first value of k (`m=1`) the results are sorted in the order described before, using different conditions and an index vector J, to assure that no value could occur twice.

```
%------Definition of the order in the first solution -----%
if m == 1
   mode1 = find( real(r(:,1)) > 1.5);
   sorted(1,1) = r(mode1,1);
   J = allindex(allindex ~= mode1);

   mode2 = find( real(r(J,1)) < -1.5);
   sorted(2,1) = r(J(mode2),1);
   J = J(J ~= J(mode2));

   [~, lasermode] = min( abs(1 - (1./real(r(J,1)) )));
   sorted(3,1) = r(J(lasermode),1);
   J = J(J ~= J(lasermode));

   [~, antilasermode] = min(abs(1+(1./real(r(J,1)))));
   sorted(4,1) = r(J(antilasermode),1);
   J = J(J ~= J(antilasermode));

   [~, plasmamode] = min( abs(1-(wp./real(r(J,1)))));
   sorted(6,1) = r(J(plasmamode),1);
   J = J(J ~= J(plasmamode));

   [~, antiplasmamode] = min( abs(1+(wp./real(r(J,1)))));
```

```
   sorted(5,1) = r(J(antiplasmamode),1);
   J = J(J ~= J(antiplasmamode));

   sorted([7,8],1) = r(J,1);
```

Now proceeding to all further columns of `r`. Using a loop (`for g = 1:1:8`) for every entry of the row determined at `m-1`, one finds the corresponding value in the right now calculated roots. A switch-case structure, based on the index of the row which is sorted, is used to improve the speed of the procedure because of investigating different r arrays lead to following results. It can be seen that the laser mode stays nearby 1, and the two first modes are mostly easy identifiable. Therefore the sorting of this values follows the same procedure (`case1, 2, 3, 4`). The algorithm takes the specified cell of the sorted array(`sorted(g,m-1)`), then, using the find command, those cells in `r(g,m)` are matched, if the difference of both real parts is smaller than 0.05. If more than one value fulfills the condition, a second condition finds the solution with the smaller difference in the imaginary parts. The identified entry is then stored into `sorted(g,m)` and its index is removed from the indexing vector `J`.

```
switch g
case {1, 2, 3, 4}
I = find( ((abs( real(sorted(g, m-1)) - (real(r(J, m))) )) < 0.05));

if numel(I) > 1
  diim = min( abs( imag(sorted(g, m-1)) - (imag(r(J(I), m))) ));
new = find( abs( imag(sorted(g, m-1)) - (imag(r(J(I), m))) ) == diim);
M = I(new);
  sorted(g, m) = r(J(M),m);
  index(g) = J(M);
J = J(J ~= J(M));

    else
sorted(g, m) = r(J(I),m);
index(g) = J(I);
J = J(J ~= J(I));

    end
```

The matching condition for the fifths column (`case 5`) uses that only three modes have a negative imaginary part. In the rare case that two negative values are left, the minimum distance between the real part of the corresponding and the matching ones is determined.

```
case 5
  I = find( real(r(J,m))<0);
```

```
  if numel(I) > 1
H = find( min( abs( real(sorted(g,m-1)) -real( r(I,m)))));
sorted(g, m) = r(J(I(H)),m);
index(g) = J(I(H));
J = J(J ~= J(I(H)));

  else
    sorted(g, m) = r(J(I),m);
index(g) = J(I);
J = J(J ~= J(I));
  end
```

`case 6` has the special, that one of the modes beginning at 0 grows and the real parts of them cross as well as the imaginary parts. For the seventh column the same procedure is followed. Firstly the algorithm controls if the real parts of the remaining entris are nearby. If this occurs, it picks the value with the lowest distance, taking care about imaginary as well as real part. If this is not, it finds the entry with the minimum distance in the real part as well as the second minimum. If the second minimum is nearby the minimum, it takes a look at the imaginary parts and compares the distances. There is a double check, that if both, imaginary and real part of two entrys are close to each other, it takes the original value.

```
case 6,7

if (abs(real(sorted(g, m-1))-(real(r(J, m))))<1e-3) == logical([1 1 1]')
  [~, I] = min( abs( (sorted(g, m-1)) - ((r(J, m))) ));
  sorted(g, m) = r(J(I),m);
  index(g) = J(I);
  J = J(J ~= J(I));
else
     [~, I] = min( abs( real(sorted(g, m-1)) - (real(r(J, m))) ));
     T = J( J ~= J(I));
     [~, K] = min( abs( real(sorted(g, m-1)) - (real(r(T, m))) ));
  if (abs(1-real(r(T(K),m))/real(r(J(I),m)))<0.1
      && abs(imag(sorted(g, m-1)))>1e-10)
 [diim, M] = (min(abs(imag(sorted(g, m-1))
   -(imag(r([J(I);T(K)],m)))));)
     if M ==1
       sorted(g, m) = r(J(I),m);
       index(g) = J(I);
       J = J(J ~= J(I));
     else
       if abs(1- (imag(r(J(I), m)))/ diim) < 0.1
```

```
          sorted(g, m) = r(J(I),m);
          index(g) = J(I);
      J = J(J ~= J(I));
        else
          sorted(g, m) = r(T(K),m);
          index(g) = T(K);
          J = J(J ~= T(K));
   end
    end
  else
    sorted(g, m) = r(J(I),m);
    index(g) = J(I);
    J = J(J ~= J(I));
  end
end
```

The last entry is the one which was not used before.

```
case 8
  sorted(g, m) = r(J, m);
  index(g) = J;
```

Erklärung

Ich versichere, dass ich diese Arbeit selbstständig verfasst und keine anderen als die angegebenen Quellen und Hilfsmittel benutzt habe.

Heidelberg, den 8. Mai 2018